Multichannel Adaptive Enhancement of the Electrogastrogram

JIANDE CHEN, JOOS VANDEWALLE, SENIOR MEMBER, IEEE, WILLY SANSEN, SENIOR MEMBER, IEEE, GASTON VANTRAPPEN, AND JOZEF JANSSENS

Abstract—**The electrogastric signal can be measured cutaneously on the abdomen. This is attractive because it is harmless to patients or volunteers. However, the poor quality of the cutaneous measurements necessitates signal enhancements. Hence, in this paper, an adaptive multichannel signal enhancing system is proposed. The μ-vector least mean square (LMS) algorithm is applied to adjust the weights of the adaptive filters in the system. The detailed description and the performance analysis of the system is given in the paper.**

Applying the proposed system, the respiratory artifact, the electrode-skin noise, some of motion artifacts, and the electrocardiography (ECG) can be efficiently reduced while the characteristics of the relevant gastric signal is less affected.

I. Introduction

THE ELECTROGASTRIC signal can be measured cutaneously by attaching electrodes to the abdominal skin. The recorded cutaneous gastric signal is often called the electrogastrogram (EGG) [16]. Since the first measurements made in 1922 [1] a great deal of research effort has been spent on the cutaneous EGG since it is noninvasive and harmless to patients or volunteers. Compared with other electrophysiological measurements, such as electrocardiography (ECG) and electroencephalography (EEG), however, the progress of the applicability of the methods has been very slow. One of the most important reasons is that the cutaneous EGG contains considerable noise.

Signal processing techniques which have been applied to improve the quality of the EGG or to extract relevant information from the EGG include bandpass filtering [11], [14], [17], fast Fourier transform [3], [20], [21], phase-lock filtering [15], autocorrelation [2], autoregressive modeling [13], and adaptive filtering [5]–[8], [12], [19].

This paper presents an adaptive method for the enhancement of the gastric signal component in the EGG. It is structured as follows. In Section II we describe the method of the measurement and the characteristics of the EGG. Section III introduces the principles of the adaptive signal enhancement. The adaptive system for the enhancement of the human EGG is presented in Section IV. In Section V, the performance of the proposed adaptive enhancing system on simulations is investigated. In Section VI, the performance of the system on EGG signals is discussed and one application is described.

Manuscript received June 6, 1988; revised August 11, 1989.

J. Chen was with the Department of Electrical Engineering, Katholieke Universiteit Leuven, Belgium. He is now with the Department of Internal Medicine, University of Virginia, Charlottesville, VA 22908.

J. Vandewalle and W. Sansen are with Lab. ESAT, Department of Electrical Engineering, Katholieke Universiteit Leuven, Kard. Mercierlaan 94 3030 Leuven, Belgium.

G. Vantrappen and J. Janssens are with the Department of Medical Research, Campus Gasthuisberg, Katholieke Universiteit Leuven, 3000 Leuven, Belgium.

IEEE Log Number 8933064.

II. The Measurement and Characteristics of the EGG

Healthy volunteers, who fasted over night, are asked to lie on their back and to keep as still as possible. Ag/AgCl (red dot, 3M) electrodes (commonly used for the measurement of the ECG) are attached on the abdomen. Bipolar signals are derived by connecting the electrodes in pairs. All bipolar signals are amplified by Universal Amplifier 854 with cutoff frequency of 5 Hz (it should be mentioned here that the cutoff frequency could be set lower, but the lower cutoff frequency is not available in our recording equipment) and are stored on an analog tape by a tape recorder (TEAC). The recorded signals are then digitized by a 8 channel 12-bit A/D converter with a sampling frequency of 12 Hz. Right after the A/D conversion a digital lowpass filter with cutoff frequency of 1 Hz (or 0.5 Hz) is applied and the signal is sampled again with a frequency of 2 Hz.

Fig. 1 shows a bipolar cutaneous EGG measured from a normal fasted volunteer. The slow wave (its period equals to about 20 s) is the gastric signal component, the spike-like activity is the ECG, and the superimposed sinusoidal disturbance is the respiratory artifact. Fig. 2 is the power spectrum of the signal (512 s) shown in Fig. 1. The lowest frequency at about 0.05 Hz shows the gastric signal and the second peak from the left around 0.3 Hz is caused by the respiratory artifact. The frequency of the ECG is not shown in this figure. It is about 1 Hz or higher.

From these two figures we see that the EGG is a mixture of the gastric signal and of noise. Generally, noise consists of the respiratory artifact, the ECG, the noise resulting from electrode–skin interface [18], motion artifacts, and other possible unknown noise. The frequencies of different components in the EGG are listed in Table I. The frequency of the gastric signal component is very low,

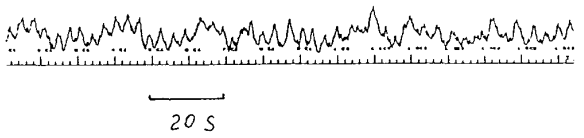

Fig. 1. Cutaneous EGG measurement. Slow wave; gastric signal; fast wave; respiratory artifact; spike activities: ECG.

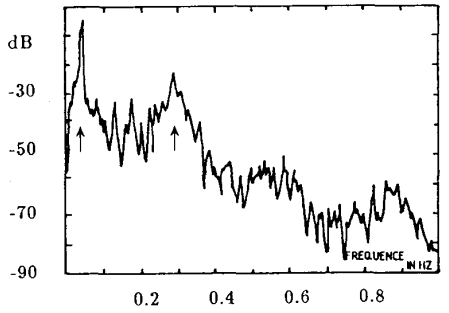

Fig. 2. Power spectrum (dB) of the EGG (512 s data, low-pass filtered with cutoff frequency of 1 Hz). First peak (marked with an arrow) from left shows the gastric signal; second peak (marked with another arrow) from left shows the respiratory artifact.

TABLE I
COMPOSITIONS OF THE EGG SIGNAL

	Component	*Frequency (Hz)*
Interested component	Gastric signal component	0.05
Noise	Respiratory disturbance	0.2–0.4
	Electrocardiography	0.8–1.0
	Electrode-skin noise	less than 0.03
	Motion artifacts	whole range
	Other possible noise	unknown

0.05 Hz or 3 cycles/min. However, the frequencies higher than 6 cycles/min and lower than 2 cycles/min have also been observed [9], [20].

The characteristics of the EGG are summarized as follows. First, the gastric signal in the EGG at certain time is a weighted summation of all the internal electrogastric activities at that time. Its waveform is related to the position of the electrodes and to the activity of the stomach, such as the contraction of the stomach. Second, the fundamental frequency of the gastric signal is about 0.05 Hz. Its waveform is not sinusoidal. This means that the gastric signal may have harmonics or some other higher frequency components. Fig. 3 shows a portion of a 2 h EGG measured from another volunteer, from which we can be convinced that the gastric signal is not sinusoidal. Moreover in some situations, such as in the tachygastria case, the frequency of the EGG can be much higher. Fig. 4 present the power spectra of a tachygastria EGG (512 s). We can see from this figure both the normal frequency (about 0.05 Hz) and the higher frequency (see peak at about 0.17 Hz). Third, the EGG contains considerable noise. Some noise, such as motion artifacts, are within the frequency range of the gastric signal. Fourth, the amplitude and the frequency of the gastric signal component change from time to time according to our experience. Hence, the EGG is a nonstationary signal. Moreover, different positions of the electrodes result in different waveforms.

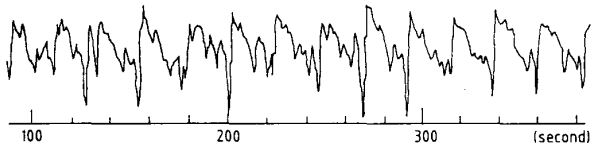

Fig. 3. Nonsinusoidal cutaneous EGG measurement. The waveform of the EGG is not sinusoidal. This means the gastric signal has harmonics, i.e., higher frequency components other than the fundamental frequency exist.

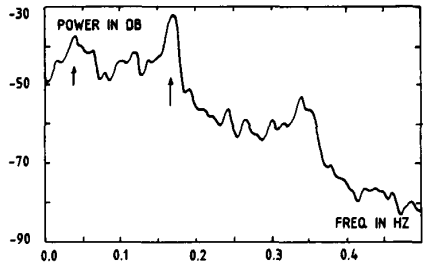

Fig. 4. Power spectrum (dB) of an tachygastria EGG (512 s data low-pass filtered with cutoff frequency of 0.5 Hz). First peak (marked with an arrow) from left shows the normal gastric signal; Second peak (marked with another arrow) shows the higher frequency of the gastric signal.

Based on the characteristics of the EGG we propose in the following sections an adaptive signal enhancing system for the human EGG. It performs well in most situations except in the case where the fundamental frequency of the gastric signal overlaps with that of the respiratory artifact. If this exceptional case occurs the adaptive system for the cancellation of the respiratory artifact proposed in [8] is especially suited.

III. Principles of Adaptive Signal Enhancing

Fig. 5 shows a least mean square (LMS) adaptive signal enhancer [10]. The primary input d_j contains signal s_{0j} and noise n_{0j}. They are assumed to be uncorrelated with each other. The reference input x_j contains noise n_{1j} and signal s_{1j} related to s_{0j} but not necessarily the same waveform as s_{0j}. n_{0j} is assumed to be uncorrelated with either of s_{0j}, n_{1j} and s_{1j}.

The output y_j of the adaptive filter is expressed as

$$y_j = \sum_{k=1}^{N} w_{kj} x_{j-k} \tag{1}$$

and the residual error between the filter output and the primary input can be written as

$$e_j = d_j - y_j. \tag{2}$$

The weight vector of the adaptive filter at time $j+1$ is adapted according to the LMS algorithm [22] as follows:

$$W_{j+1} = W_j + 2\mu e_j X_j \tag{3}$$

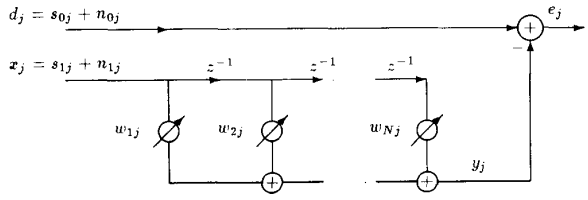

Fig. 5. LMS adaptive signal enhancer. Among s_{0j}, n_{0j}, s_{1j}, n_{1j}, only s_{1j} and s_{0j} are correlated with each other.

with

$$X_j = [x_j, x_{j-1}, \cdots, x_{j-N+1}]^T \tag{4}$$

$$W_j = [w_{1j}, w_{2j}, \cdots, w_{Nj}]^T \tag{5}$$

where x_j is the reference signal at time instant j, w_{kj} ($k = 1, 2, \cdots, N$) are the kth coefficients of the adaptive filter at time j, N is the length of the adaptive filter and μ is a constant called feedback factor which determines the convergence speed of the adaptation.

After the convergence of the adaptive filter the mean squared value of the error signal e_j is minimal and the output of the adaptive filter, y_j is a best estimate of the signal s_{0j} in the primary input in the sense of the mean square error. As shown in the adaptive filter literature [10], the filter output is a best estimate of signal s_0 in the sense of mean square error. More generally, *the adaptive filter generates a replica of that part of the primary input which is correlated with the reference input (or input to the adaptive filter).* This conclusion is a key to understand the adaptive signal enhancing system to be proposed in the next sections.

The adaptive signal enhancing system shown in Fig. 5 can be called a two-channel adaptive signal enhancer, and a multichannel adaptive signal enhancing system is shown in Fig. 6 (time index j is omitted for simplicity). The primary input d_j contains a desired signal s_0 and noise n_0. Every reference input consists of a signal s_k correlated to s_0 and noise n_k uncorrelated to either of s_0 and n_0. The signals s_k ($k = 1, m$) in the reference inputs need not have the same waveform as the signal s_0 in the primary input. As explained in previous paragraph the output of the system, y is a best estimate of s_0 in the primary input.

It has been proved by Ferrara and Widrow [10] that *the more reference inputs are available which contain correlated signal components, the better the system performance will be.*

If the reference input x_j in Fig. 5(a) is derived from the primary input d_j by only inserting a delay Δ, the system is called an *adaptive line enhancer* (ALE) (see Fig. 7). Assume the input to the ALE consists of a correlated signal s_j, such as periodic signal, and uncorrelated noise n_j. The only difference between the primary and the reference inputs is the delay Δ. If the delay is chosen such that the noise $n_{j-\Delta}$ in the reference input becomes uncorrelated with n_j in the primary input, then the output of the adaptive contains signal s_j alone after the convergence of the

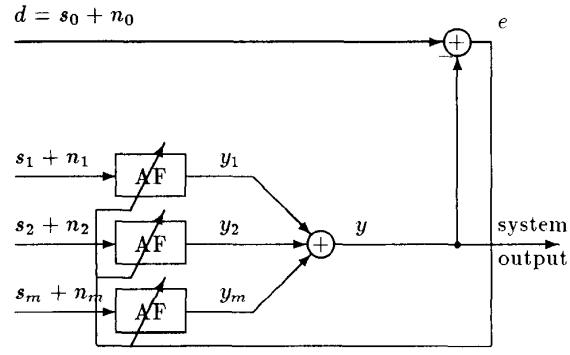

Fig. 6. Multichannel adaptive signal enhancer. Primary input: $s_0 + n_0$, s_0 is the signal to be extracted; reference inputs: $s_1 + n_1, \cdots, s_m + n_m$. AF: adaptive filter. Time index j is omitted.

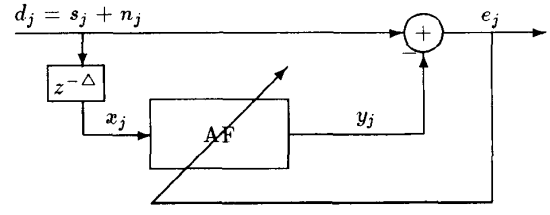

Fig. 7. Adaptive line enhancer. AF: adaptive filter, $z^{-\Delta}$: Δ samples delay. Δ is used to decorrelate noise, n_j (if not periodic) in the primary input.

adaptive algorithm. It can be explained as follows. Under the above assumptions there is an M such that (7) holds.

$$d_j = s_j + n_j$$

$$x_j = s_{j-\Delta} + n_{j-\Delta}$$

$$E[s_j s_{j-k}] \neq 0 \qquad \text{for any } k \tag{6}$$

$$E[n_j n_{j-k}] = 0 \qquad \text{for } k \geq M. \tag{7}$$

Choosing the delay equal (or larger) to M, $\Delta \geq M$ we can see that the noise, $n_{j-\Delta}$ in the reference input is uncorrelated with n_j in the primary input [see (7)], while the signal $s_{j-\Delta}$ is still correlated with s_j in the primary input [see (6)]. Consequently, the filter output y_j is a replica of s_j according to the observation made earlier.

IV. Adaptive Enhancement of the Human EGG

Having discussed both the characteristics of the human EGG and the adaptive signal enhancing technique, we propose an adaptive signal enhancing system for the EGG in this section. The system is shown in Fig. 8. It is composed of two stages: a preprocessing and a modified multichannel adaptive signal enhancing.

A. Preprocessing

In the second section we indicated that the EGG is a nonstationary signal and the SNR is low. So when the LMS algorithm is used the convergence speed should be fast enough to track the time variations of the EGG sta-

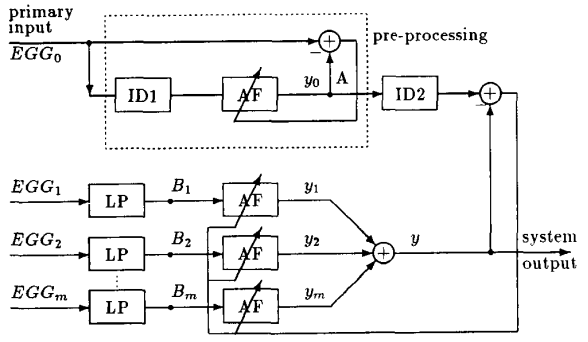

Fig. 8. Adaptive enhancing system for the human EGG. Dashed part: the preprocessing adaptive line enhancer. The rest of the system: modified multichannel signal enhancer with $EGG_1, \cdots, EGG_m$ as reference inputs. AF: adaptive filter; LP: FIR low-pass filter. ID1: the delay used to decorrelate noise. ID2: the delay used to compensate the delay introduced by the FIR low-pass filter.

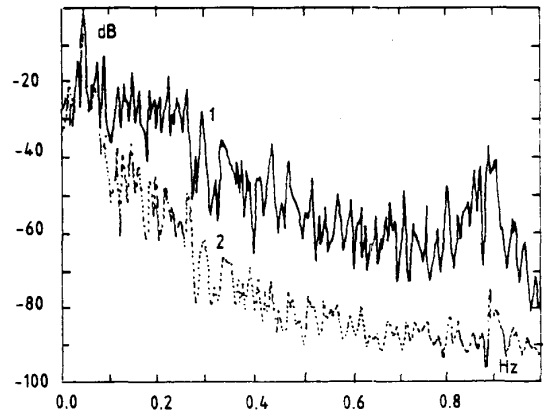

Fig. 9. Power spectra (dB) of the EGG before and after the preprocessing (512 s data). Normal line: input power spectrum; dotted line: power spectrum of the preprocessing output. Frequency components around 0.05 Hz reflect the gastric signal. It is little affected by the preprocessing. The level of noise is substantially reduced.

tistics. That is, the value of feedback factor should be larger; however, a larger μ will result in a larger contribution of gradient noise [23]. In order to keep the gradient noise within a tolerable limit when the fast adaptation is needed, an alternative way is to reduce the noise components in the input signal. For this reason the preprocessing is introduced [4].

The preprocessing (dashed part in Fig. 8) is simply an adaptive line enhancer. The input signal to the preprocessing is the EGG to be enhanced and the reference input is its delayed version. Properly choosing the length of the adaptive filter, feedback factor μ and the delay $ID1$, the output of the preprocessing y_0, after the convergence of the adaptive filter, contains little uncorrelated noise. The gastric signal is, however, not affected because it is highly correlated. The SNR of the primary signal is then considerably increased after the preprocessing, which relieves the "burden" of the next stage processing.

Fig. 9 shows the power spectra of an EGG (512 s) before and after the preprocessing. Line 1 is the power spectrum of the signal before the preprocessing and line 2 (dashed line), after the preprocessing. From the figure we can see that the gastric signal component around 0.05 Hz is little affected. The power of the noise with frequency greater than 0.1 Hz is, however, reduced by 30 dB or more.

B. Modified Multichannel Adaptive Enhancing

The remainder of the system shown in Fig. 8 is the modified multichannel adaptive enhancing. Its primary input, y_0 is the output of the preprocessing and the reference inputs EGG_1-EGG_m are different positional EGG. All of the reference inputs are first filtered by an FIR digital low-pass filter in order to eliminate the periodic respiratory artifact which is correlated with that in the primary input y_0. The delay $ID2$ is inserted in the primary input to compensate the time delay introduced by the FIR filters in the reference inputs.

"LP" in Fig. 8 is a low-pass FIR filter with cutoff frequency of 0.2 Hz. It should be higher than the fundamental frequency of the gastric signal. It may distort the waveform of the gastric signals in the input signals EGG_1 to EGG_m. But it has linear phase character so the phase character of the gastric signal component is not affected except the time delay. The adaptive filter (AF) in Fig. 8 is realized by the tapped delay line shown in Fig. 5(b). The tapping space time is one sample, that is, 0.5 s and the number of weights will be discussed later. The gastric signals in different positional EGG may have different waveform, different amplitudes, and different phases. However, they must have the same time-varying characters, such as the variations of the frequency and of the amplitude from time to time, because they all originated from the stomach.

Assume that the primary input EGG_0 contains a gastric signal, uncorrelated noise, and correlated noise (mainly the respiratory artifact). After the preprocessing at point A in the primary input we have the gastric signal and some correlated noise (mainly respiratory artifact). After low-pass filtering at points $B_1, B_2, \cdots, B_m$ we have the gastric signals related to that in the primary input and little noise mostly uncorrelated with that in y_0. Properly choosing the parameters of the system, the output y is then, after convergence, a best estimate of the gastric signal component in the primary input.

Recall that the adaptive filter generates a replica of that part of the primary input which is correlated with the reference input to the adaptive filter. From the proposed system the following conclusions can be made:

The system output y is a best estimate of the gastric signal component in the primary input. The respiratory artifact, the ECG, the electrode-skin noise and some of the motion artifacts can be efficiently reduced by the proposed system.

Although the respiratory artifact and the ECG are correlated signals, they can not be extracted from the primary input by the adaptive filters since they don't appear at the points $B_1, \cdots, B_m$.

The electrode–skin noise can be eliminated if no common reference electrode is used since this class of the noise in one EGG is uncorrelated with that in another EGG.

The motion artifacts are not periodic and thus some of these can be reduced by the preprocessing if the delay *ID*1 is properly chosen. Some which are uncorrelated in different EGG can also be reduced. The complete reduction of the motion artifacts is, however, not guaranteed by the proposed system.

C. System Parameters

Several parameters need to be determined in the system shown in Fig. 8. They are feedback factor μ, the length of the adaptive filter and the delay units, *ID*1 and *ID*2. The most crucial parameter is *the feedback factor* μ. The necessary and sufficient condition for the convergence of the LMS algorithm is as follows [22]:

$$1/\sigma^2 > \mu > 0 \tag{8}$$

where σ^2 is the total input power to the adaptive filter.

Since the EGG is a nonstationary signal, the μ-vector LMS algorithm proposed in [4] is used for all of the adaptive filters in the system. It is described as follows:

$$W_{j+1} = W_j + 2\vec{\mu}_j e_j X_j \tag{9}$$

$$\vec{\mu}_j = \text{diag}[\mu_{1j}, \mu_{2j}, \cdots, \mu_{ij}, \cdots \mu_{Nj}] \tag{10}$$

$$\mu_{ij} = (1-\alpha)^{i-1} q_j \tag{11}$$

$$q_j = \mu/(\sigma_j^2 + \sigma_0^2) \tag{12}$$

$$\sigma_j^2 = (1-\beta)\sigma_{j-1}^2 + \beta x_j^2 \tag{13}$$

where α is a nonstationary factor (or forgetting factor) less than 1. Observe that α should be determined according to the variation degree of the input statistics; for stationary input α could be chosen to be zero. q_j is the normalized feedback factor which is given to the most recent tap. μ is the factor controlling the convergence of the algorithm. σ_j^2 is an estimate of the total input energy to the adaptive filter. σ_0^2 is a small constant used to prevent μ_{ij} from getting too large when the input signal gets very small. β is a small constant less than 1, generally equal to $1/N$.

In general faster adaptation (large value of μ) leads to more noisy adaptation processes. When the input environment is statistically stationary the best steady-state performance results from slow adaptation. In the EGG application, however, the input statistics is time-varying. Hence a fast adaptation is needed in order to follow the time variations of the signals.

The *length of the tapped delay line*, namely the number of adaptive weights, should be at least the reciprocal of the desired filter resolution [22]. Since the normal period of the gastric signal is 20 s (40 samples), this value is usually chosen to be 60 in the experiments. The *delay ID*1 is used to decorrelate the noise in the primary input. For white noise it can be set to be 1. For the EGG application we have found that if the motion artifacts are not strong the change of its value within a certain range does not affect the system performance. It is usually chosen to be 1. The delay *ID*2 is inserted to compensate the delay introduced by the FIR filters.

V. Performance Analysis Based on Simulations

To investigate the performance of the proposed system quantitatively, simulations have been conducted based on the following experiments.

The input signals to the system shown in Fig. 8 (only two channels are considered) are generated as

$$\text{EGG}_{0j} = s_j + br_j + cn_j \tag{14}$$

$$\text{EGG}_{1j} = s_{1j} + br_{1j} + cn_{1j} \tag{15}$$

where r_j and r_{1j} are simulated respiratory artifacts. They are sinusoids with a frequency of 0.3 Hz. n_j and n_{1j} are uniformly distributed $(-0.5, 0.5)$ random noise. s_j and s_{1j} are simulated gastric signals in the primary input and in the reference input, respectively. They are nonstationary.

s_j is a sequence of sinus signals

$$s_j = \tilde{a} \sin(2\pi \tilde{f}_s j) \tag{16}$$

each considered over one full period. The amplitude $\tilde{a}$ and the frequency $\tilde{f}_s$ of each sinusoid vary as follows:

$$\tilde{a} = a(1 + d_a n') \tag{17}$$

$$\tilde{f} = f_s(1 + d_f n') \tag{18}$$

where n' is a white noise, having the same nature as n_j and n_{1j}. Parameters a, b, and c in (18), (19), and (22) are constants controlling the SNR of the simulated signals. d_a and d_f are nonstationary factors determining the variation degree of the frequency and of the amplitude of the gastric signal, respectively. When they are equal to zero, the gastric signal s_j turns out to be a sinusoid.

s_{1j} has different variations from s_j, but its frequency follows the same changes as s_j. It is also a sequence of sinus signals

$$s_{1j} = \sin(\pi \tilde{f}_s j) \tag{19}$$

but each considered over half a period.

Fig. 10(a) and (b) show the simulated gastric signals s_j and s_{1j}, respectively. The simulated primary input EGG_0 is shown in Fig. 10(c) (SNR = −7.8 dB).

To give some quantitative measures on the performance of the proposed adaptive system, we define terms, "mean square error" (MSE_j) and "misadjustment" (M) as follows:

$$\text{MSE}_j = E[(s_j - y_j)^2] \tag{20}$$

$$M = \frac{\sum_{j=K}^{K+L} (s_j - y_j)^2}{\sum_{j=K}^{K+L} s_j^2} \tag{21}$$

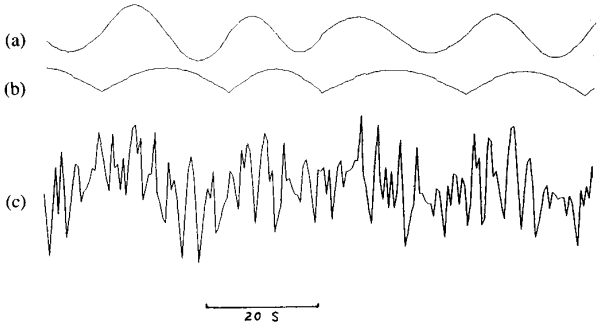

Fig. 10. Simulated nonstationary signals. (a) Simulated gastric signal in the primary input; (b) simulated gastric signal in the reference input. They have different waveform, but follow the same changes of the frequency. (c) Simulated primary input (SNR = −7.8).

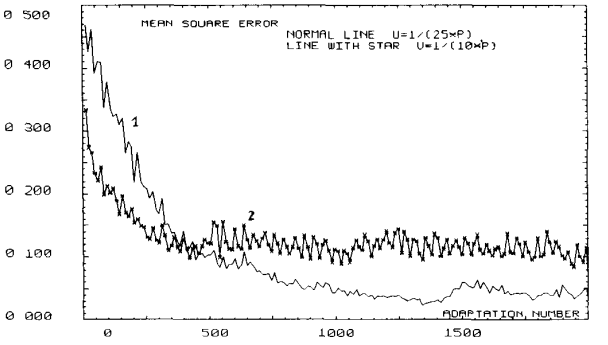

Fig. 11. Convergence of the adaptive system (mean square error versus adaptation number over 100 independent runs). $d_a = d_v = 0.5$, SNR = −7.8; $\alpha = 0.0$; curve 1: $\mu = 0.04$; curve 2: $\mu = 0.1$.

where s_j is the gastric signal in the primary input EGG_0 and y_j is the system output. The misadjustment M is an averaged relative square error in the steady state. K should be large enough such that after K adaptations, the system has already converged.

In the following experiments, the parameters are chosen as follows (if not specially mentioned):

Sample frequency: 2 Hz; length of the adaptive filters $N = 60$; order of the FIR low-pass filters: 50; cutoff frequency of the FIR low-pass filter: 0.2 Hz;

$$f_s = 0.05 \text{ Hz}, \quad f_r(\text{frequency of respiration}) = 0.3,$$

$$ID1 = 1, \quad ID2 = 25, \quad d_a = d_v = 0.5,$$

$$\text{SNR} = -7.8, \quad \mu = 0.04, \quad \alpha = 0.04.$$

A. Convergence of the System

Fig. 11 shows the convergence of the system with the stationary inputs ($d_a = d_f = 0$), the mean square error, MSE_j versus the number of the adaptations over 100 independent runs. The feedback factor μ is chosen to be 0.04 for curve 1 and 0.1 for curve 2. From these two curves we can see that for the stationary inputs, larger μ results in faster convergence and larger mean square error in the steady state. Smaller μ, on the other hand, results in slower convergence and better performance.

For nonstationary inputs, however, this is not always the case since the system has to follow the changes of the input signals. Smaller μ may result in worse performance, as shown in Table II, where $d_a = d_f = 0.5$. The first row on the table shows different values of μ and the second, the misadjustment, M in the steady state. It can be observed that for the nonstationary inputs smaller μ does not lead to better performance. The optimum value of μ for the simulated nonstationary inputs with $d_a = d_f = 0.5$ is 0.1–0.2.

B. Optimization of the μ-Vector LMS Algorithm

Table III shows the performance of the system with different values of α ($d_a = d_v = 0.5$). It can be seen in the table that for $d_a = d_f = 0.5$, the optimum value of α is equal to 0.6, which leads to a minimum misadjustment.

TABLE II
EFFECT OF μ ON THE SYSTEM PERFORMANCE WITH NONSTATIONARY INPUTS ($d_a = d_f = 0.5$, $\alpha = 0.04$, SNR = −7.8 dB)

feedback factor, μ	0.005	0.01	0.02	0.04	0.1	0.2
Misadjustment, M	0.630	0.473	0.417	0.398	0.357	0.358

TABLE III
EFFECT OF α ON THE SYSTEM PERFORMANCE ($d_a = d_f = 0.5$, $\mu = 0.2$ SNR = −7.8 dB)

Nonstationary factor, α	0.8	0.6	0.4	0.4	0.0
Misadjustment, M	0.359	0.343	0.357	0.462	0.788

Fig. 12 shows the performance of the system with different α in the frequency domain. Curve 1 is the power spectrum of the primary input (512 s data). Curve 2 and 3 are the system outputs with $\alpha = 0$ and $\alpha = 0.04$, respectively. From this figure we can see that the power of the simulated gastric signal is little affected by the system: 2.5 dB reduction for the maximum value with $\alpha = 0$; 3.5 dB with $\alpha = 0.04$. The power of the respiratory artifact and the white noise is substantially reduced: 44 dB reduction of the maximum power of the respiratory artifact with $\alpha = 0$ and 59 dB reduction with $\alpha = 0.04$. The noise level is reduced by about 55 dB. We can also observe that better performance (15 dB more reduction of the respiratory artifact) is achieved by the μ-vector LMS algorithm.

C. Effect of the SNR

Experiments with different SNR of the primary input have been conducted and the results are shown in Table IV. It can be seen that as the SNR of the input signal increases the misadjustment gets smaller and smaller, i.e., better performance can be obtained with higher SNR.

D. Nonstationary Effect

We have shown in Fig. 11 and that with stationary inputs better performance can always be achieved by choosing smaller μ. With nonstationary inputs this is not always true. Optimum values of α can be found for different non-

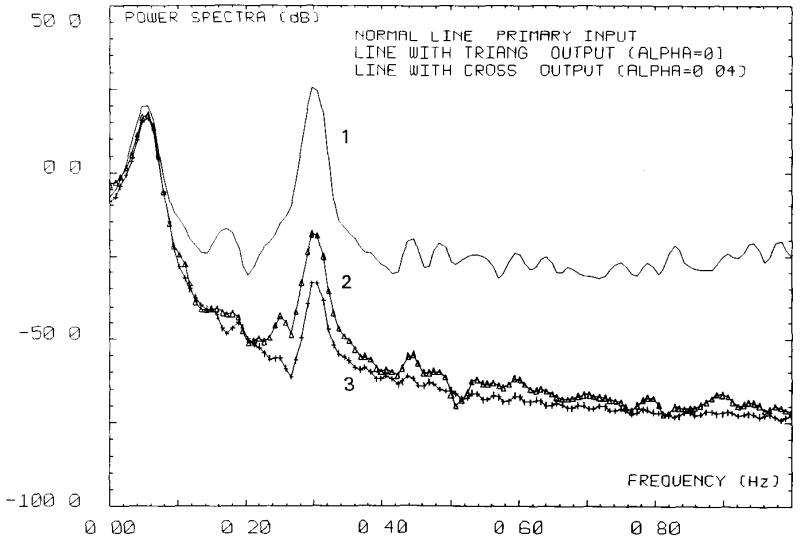

Fig. 12. Power spectra (dB) of the primary input and the system outputs with different values of α (512 s data). $d_a = d_f = 0.5$, $\mu = 0.04$, SNR $= -7.8$. Curve 1: primary input, First peak from the left shows the gastric signal and the second peak from the left, the respiratory artifact; curve 2: system output with $\alpha = 0.0$; curve 3: system output with $\alpha = 0.04$.

TABLE IV
EFFECT OF SNR OF THE PRIMARY INPUT ON THE SYSTEM PERFORMANCE ($d_a = d_f = 0.5$, $\mu = 0.04$, alpha = 0.04)

Signal-to-noise Ratio, SNR (dB)	−16.7	−7.8	−1.2	10.8	17.8
Misadjustment, M	0.708	0.398	0.157	0.149	0.148

TABLE V
EFFECT OF TIME VARIATIONS OF THE FREQUENCY AND THE AMPLITUDE OF THE SIGNAL ON THE SYSTEM PERFORMANCE ($\mu = 0.04$, $\alpha = 0.04$, SNR $= -7.8$ dB)

Time variation degree, d_a, d_f	0.7	0.5	0.3	0.2	0.1	0.0
Misadjustment, M	0.488	0.398	0.319	0.398	0.414	0.2

stationary signals. To see this several experiments have been done. In Table V we fix the value of α ($= 0.04$), but vary the parameters d_a and d_f. From the table we can see that $\alpha = 0.04$ is more suitable for $d_a = d_f = 0.3$ than for others. When the deviations of the frequency and of the amplitude of the signal are further away from 0.3, the performance of the system with $\alpha = 0.04$ becomes worse. The last column in the table means that the input signals are stationary and thus the best performance is obtained.

E. Effect of the Preprocessing

Fig. 9 has already shown the performance of the preprocessing. It is known that some uncorrelated noise (not necessarily white noise as in the simulations) can be reduced by the preprocessing. Fig. 13 presents the improvement achieved by the preprocessing for the simulated signals. Curve 1 is the power spectrum (512 s data) of the system output without the preprocessing and curve 2 is that with the preprocessing. From the figure it is clear that the power of the simulated gastric signal and the simulated respiratory artifact is not affected by the pre-processing but more white noise reduction is obtained by the preprocessing.

It should be noted that in most of the above experiments worst case conditions were simulated: very low SNR

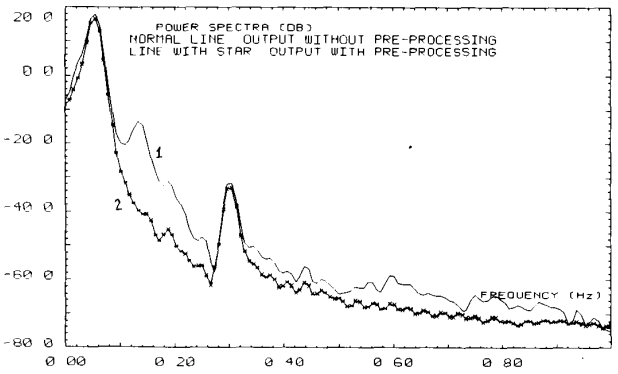

Fig. 13. Power spectra (dB) of the system outputs with and without the preprocessing (512 s data). Curve 1: the output without the preprocessing; curve 2: the output with the preprocessing.

(-7.8 dB); big changes of the frequency and the amplitude of the gastric signal (50% deviations); bad reference signal (the waveform of the gastric signal, s_{1j} in the reference input is completely different from that, s_j, in the primary input).

In reality, however, the SNR is normally higher than -7.8 dB, the time variations of the gastric signal may not

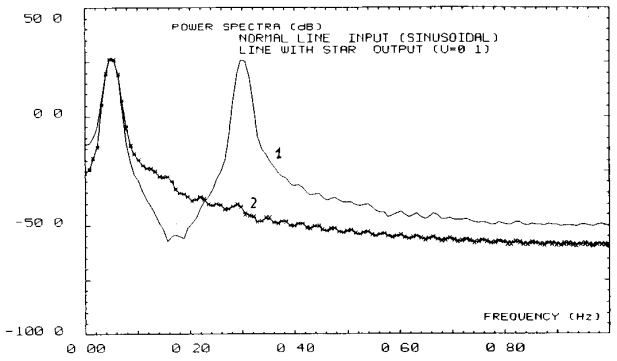

Fig. 14. Power spectra (dB) of the primary input and the system output (512 s data) under following conditions: $d_a = d_f = 0.0$, $\mu = 0.01$, SNR $= -1.1$. Curve 1: primary input; curve 2: system output. It can be seen that with the stationary inputs the noise (obviously for the respiratory artifact) can be completely eliminated.

Fig. 15. Waveform of the gastric signal in the primary input and the system output under the same conditions as those in Fig. 14. Little waveform distortion of the gastric signal can be observed.

be so fast and the waveform of the gastric signals in different EGG recordings are more similar with each other than in the above simulations.

Assuming better conditions, $d_a = d_f = 0$, SNR $= -1.1$, and choosing a smaller $\mu (= 0.01)$, we have conducted one more experiment. The results are shown in Figs. 14 and 15. Fig. 14 shows the power spectra of the primary input (curve 1) and the system output (curve 2). It is seen that the gastric signal is hardly affected while the respiratory artifact and the white noise are significantly reduced. In Fig. 15 we present the original gastric signal in the primary input and the system output in time domain, from which we can see that the waveform of the gastric signal is little affected.

VI. Performance on EGG Signals

The proposed adaptive signal enhancing system has been successfully used for real cutaneous gastric signal processing. Our experiments with more than 15 measurements (each more than 1 h) have shown that the system is efficient and is simple to use or to implement.

With sampling frequency of 2 Hz, following suitable values have been found: the length of the adaptive filter, $N = 50$–60; the feedback factor, $\mu = 0.06$; and the nonstationary factor, $\alpha = 0.04$.

Fig. 16 shows one of the results. Fig. 16(a)–(d) show four different positional EGG's and Fig. 16(e) and (f) are the adaptive enhancing outputs of the signal EGG_0. In Fig. 16(e) only EGG_1 is used as the reference input and in Fig. 16(f), three reference inputs EGG_1, EGG_2, and EGG_3 are used. The improvement of the system output quality by

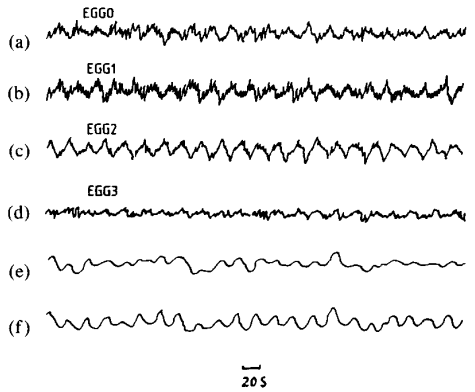

Fig. 16. Adaptive enhanced result of the human EGG (512 s data). (a) The primary input (EGG_0); (b)–(d) the reference inputs (EGG_1–EGG_3); (e) system output with EGG_1 as the reference; (f) system output using all the reference EGG signals.

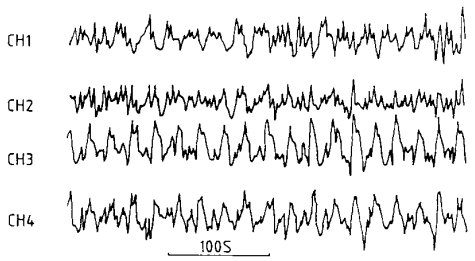

Fig. 17. Four-channel EGG signals measured on the abdomen along the vertical axis of the stomach (low-pass filtered with cutoff frequency of 0.5 Hz).

using more reference inputs can be seen by comparing Fig. 16(e) and (f).

Applying the adaptive system in this paper, the SNR of EGG signals can significantly be improved. This makes the direct waveform analysis of the EGG easier, and more information can be extracted from the EGG, such as the changes of the frequency and of the amplitude of the gastric signal, the different patterns of the EGG waveform associated to different subjects (if there are any) and so on.

In order to illustrate the applicability of the method, we apply the method on the detection of the propagation of the gastric activity from the EGG [9]. Fig. 17 shows four channel EGG recorded from a patient by locating four electrodes on the abdomen along the vertical axis of the stomach. Each of these is connected to a common referencing electrode also attached on the abdominal skin. The EGG shown in Fig. 17 have been lowpass filtered with cutoff frequency of 0.5 Hz. Fig. 18 shows the adaptively enhanced outputs by using the system in this paper. From this figure phase shifts among the different channels can be clearly observed. A method for the precise calculation of the phase shifts among the EGG's can be found in [9].

VII. Conclusion

In this paper we described the measurement of the EGG and analyzed the characteristics of the EGG. Based on

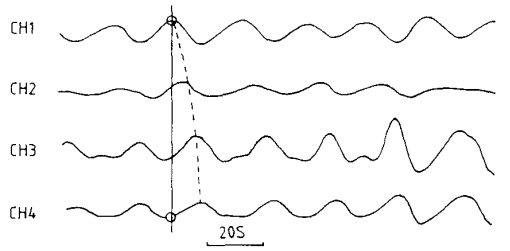

Fig. 18. A portion of the adaptive enhanced EGG signals of those shown in Fig. 17. Phase shifts among the EGG signals can be clearly observed.

this an adaptive signal enhancing system is proposed for the human EGG.

The performance of the proposed system has been thoroughly investigated. It has been shown that the system can substantially reduce the respiratory artifact, the ECG, the noise resulting from electrode–skin interface and some motion artifacts. The gastric signal component in the EGG is, however little affected by the system. Consequently, the signal-to-noise ratio of the EGG can be significantly improved.

REFERENCES

[1] W. C. Alvarez, "The electrogastrogram and what it shows," *J. Amer. Med. Assoc.*, vol. 78, pp. 1116–1118, 1922.
[2] B. H. Brown *et al.*, "Auto-correlation and visual analysis," *Med. Biol. Eng.*, vol. 9, pp. 305–314, 1971.
[3] B. H. Brown, R. H. Smallwood, H. L. Duthie, and C. J. Stoddard, "Intestinal smooth muscle electrical potentials recorded from surface electrodes," *Med. Biol. Eng.*, vol. 13, pp. 97–102, 1975.
[4] J. Chen and J. Vandewalle, "An μ-vector LMS adaptive system for enhancing nonstationary narrow band signals," in *Proc. IEEE Int. Conf. Circuit Syst.*, 1988, pp. 771–774.
[5] J. Chen, J. Vandewalle, W. Sansen, G. Vantrappen, and J. Janssens, "Adaptive cancellation of respiratory disturbance in electrogastric signals," in *Digital Signal Processing*, V. Cappellini and A. G. Constantinides, Eds. North-Holland 1987, pp. 901–905.
[6] ——, "Adaptive enhancement of human electrogastrography," in *Proc. IEEE Int. Conf. Biomed. Eng.*, Boston, MA, 1987, pp. 858–859.
[7] ——, "Detection of gastric signals from cutaneous abdominal measurements," in *Analysis and Optimization of Systems*, A. Bensoussan and J. L. Lions, Eds. New York: Springer, 1988, pp. 1117–1128.
[8] ——, "Adaptive method for cancellation of respiratory artefact in electrogastric measurements," *Med. Biol. Eng. Comp.*, vol. 27, pp. 57–63, 1989.
[9] J. Chen, J. Vandewalle, W. Sansen, E. Vancutsem, G. Vantrappen, and J. Janssens, "Observation of the propagation of human electrogastric activity from cutaneous recordings," *Med. Biol. Eng. Comp.*, to be published.
[10] E. R. Ferrara, Jr. and B. Widrow, "Multichannel adaptive filtering for signal enhancement," *IEEE Trans. Acoust., Speech, Signal Processing*, vol. ASSP-29, no. 3, June 1981.
[11] E. N. Goodman, H. Colcher, G. M. Katz, and C. L. Damgler, "The clinical significance of the electrogastrogram," *Gastroenterol.*, vol. 29, pp. 598–607, 1955.
[12] M. A. Kentie, E. T. van der Schee, J. L. Grashius, and A. J. P. M. Smout, "Adaptive filtering of canine electrogastrographic signals—Part 1: System design," *Med. Biol. Eng. Comput.*, vol. 19, pp. 759–764, 1981.
[13] D. A. Linkens, and S. P. Datardina, "Estimation of frequencies of gastrointestinal electrical rhythms using autoregressive modelling," *Med. Biol. Eng. Comput.*, vol. 16, pp. 262–268, 1978.
[14] T. S. Nelsen and S. Kohatsu, "Clinical electrogastrography and its relationship to gastric surgery," *Amer. J. Surg.*, vol. 116, pp. 215–222, 1968.
[15] R. H. Smallwood, "Analysis of gastric electrical signals from surface electrodes using phaselock techniques," *Med. Biol. Eng. Comput.*, vol. 16, pp. 507–518, 1978.
[16] R. M. Stern and K. L. Koch, Eds., *Electrogastrography*. New York: Praeger, 1985.
[17] C. J. Stoddard, R. H. Smallwood, and H. L. Duthie, "Electrical arrythmias in the human stomach," *Gut*, vol. 22, pp. 705–712, 1981.
[18] H. W. Tam and J. G. Webster, "Minimizing electrode motion artifact by skin abrasion," *IEEE Trans. Biomed. Eng.*, vol. BME-24, Mar. 1977.
[19] E. T. van der Schee, M. A. Kentie, J. L. Grashuis, and A. J. P. M. Smout, "Adaptive filtering of canine electrogastrographic signals—Part 2: Filter performance," *Med. Biol. Eng. Comput.*, vol. 19, pp. 765–769, 1981.
[20] E. T. van der Schee and J. L. Grashuis, "Contraction-related, low-frequency components in canine electrogastrographic signals," *Amer. J. Physiol.*, vol. 245, pp. G470–G475, 1983.
[21] E. J. van der Schee and J. L. Grashuis, "Running spectrum analysis as an aid in the representation and interpretation of electrogastrographic signals," *Med. Biol. Eng. Comput.*, vol. 25, pp. 57–62, 1987.
[22] B. Widrow *et al.*, "Adaptive noise cancelling: Principles and applications," *Proc. IEEE*, vol. 63, pp. 1692–1716, Dec. 1975.
[23] B. Widrow *et al.*, "Stationary and nonstationary learning characteristics of the LMS adaptive filter," *Proc. IEEE*, vol. 64, pp. 1151–1162, Aug. 1976.

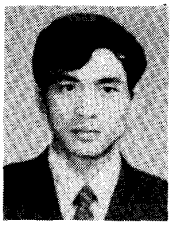

Jiande Chen was born in Zhejiang, China, on December 4, 1956. He received the B.S. degree from East China Normal University, Shanghai, China in 1982 and the Ph.D. degree in electronic engineering from Katholieke Universiteit Leuven, Belgium, in 1989 where he studied from December 1983 to May 1989.

Currently he is with Department of Internal Medicine, University of Virgina. His research interests are mainly on the adaptive signal processing and its applications in biomedical engineering and telecommunications.

Joos Vandewalle (S'71–M'79–SM'82) was born in Kortrijk, Belgium, in 1948. He received the degree of Electro-Mechanical engineer in electronics in 1971, Doctor in applied sciences in 1976, and Special Doctor in applied sciences in 1984, all at the Katholieke Universiteit Leuven.

He was a Research Associate (1976–1978) and Visiting Assistant Professor (1978–1979) at the Department of Electrical Engineering and Computer Sciences, University of California, Berkeley. He was Assistant Professor (1980–1986) and has been a Full Professor (Gewoon Hoogleraar) at the Department of Electrical Engineering, Katholieke Universiteit Leuven. Since Oct. 1980 he has been a member of the staff of the ESAT Laboratory. He has been an Academic Consultant since 1984 at the VSDM group of IMEC (Interuniversity Microelectronics Center, Leuven). He has teaching assignments in algebra, system theory, signal processing, network theory, and nonlinear systems. He is the promotor of eight completed doctoral research activities and about 13 current doctoral research activities at the KUL. His research interests are in system theory, digital signal processing, and cryptography. Special attention is devoted to the numerical aspects of the algorithms and to the use of the singular value decomposition. In these areas he has authored or coauthored more than 100 papers. He is a member of the Editorial board of *Journal A*, a quarterly journal of automatic control (1980—present) and of the *International Journal of Circuit Theory and its Applications* (1985–present).

Dr. Vandewalle received the Award of 100 Year Bell Telephone (BTMC) in 1983 and the SWIFT (Society for Worldwide Interbank Financial Telecommunication S.C.) award in 1985 (joint with Y. Desmedt and R. Govaerts). In 1986 he received the best paper award on computer aided design at the IEEE ICCD Conference, Port Chester New York (joint with L. Claesen, F. Catthoor, H. De Man, S. Note and K. Martens).

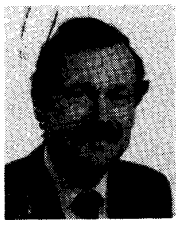

Willy Sansen (S'66-M'72-SM'86) was born in Poperinge, Belgium, on May 16, 1943. He received the engineering degree in electronics from the Katholieke Universiteit Leuven, Belgium, in 1967 and the Ph.D. degree in electronics from the University of California, Berkeley, in 1972.

In 1968 he was employed as an Assistant at the Katholieke Universiteit Leuven. In 1971 he was employed as a Teaching Fellow at the University of California. In 1972 he was appointed by the N.F.W.O. (Belgian National Foundation) as a Research Associate, at the Laboratory Elektronika, Systemen, Automatisatie, Technologie, Katholieke Universiteit Leuven where he has been full Professor since 1981. Since 1984 he has been the head of the Department of Electrical Engineering. In 1978 he spent the winter quarter as a visiting assistant professor at Stanford University, Stanford, CA, and in 1981 at the Techn. Univ. Lausanne, and in 1985 at the University of Pennsylvania, Philadelphia. His interests are in device modeling, design of integrated circuits, and medical electronics and sensors.

Dr. Sansen is a member of the Koninklijke Vlaamse Ingenieurs Vereniging (K.V.I.V.), the Audio Engineering Society (A.E.S.), the Biotelemetry Society, and Sigma Xi. In September 1969 he received a CRB Fellowship from the Belgian American Educational Foundation, in 1970 a G.T.E. Fellowship, and in 1978 a NATO Fellowship.

Gaston Vantrappen was born in 1927. He received the M.D. degree from the University of Leuven in 1953; and he specialized in internal medicine from 1953 to 1959 and received Ph.D. degree from the University of Leuven in 1961.

He is presently a Professor of Medicine of the University Hospitals of Leuven and Head of the Gastroenterologic Research Center of the University of Leuven. His main research interest is gastrointestinal motility and oesophageal disease.

Jozef Janssens was born in Merksen, Belgium, in 1943. He received the M.D. degree in surgery and obstetrics in 1968 from the Katholieke Universiteit Leuven, Belgium, and a specialization in internal medicine in 1974.

He is Adjunct Head of the Hospital St. Raphael-Gasthuisberg, Leuven Lector (since 1978) and Teaching Professor at the Department of Medicine, Katholieke Universiteit Leuven since 1979.